LBL--14174

DE82 014998

LBL-14174

FUNNY HILLS IN PION SPECTRA FROM HEAVY-ION COLLISIONS

John O. Rasmussen

Nuclear Science Division
Lawrence Berkeley Laboratory
University of California
Berkeley, CA 94720

DISCLAIMER

This work was supported by the Director, Office of Energy Research, Division of Nuclear Physics of the Office of High Energy and Nuclear Physics of the U.S. Department of Energy under Contract DE-AC03-76SF00098.

FUNNY HILLS IN PION SPECTRA FROM HEAVY-ION COLLISIONS

John O. Rasmussen
U.C. Lawrence Berkeley Laboratory

INTRODUCTION

It is indeed a pleasure to have the opportunity of discussing at this winter school some of the intriguing spectral features emerging from pion studies at the BEVALAC.

Some of the systematic features of the pion spectra have been presented to you in the earlier talk of Prof. Nagamiya. He has showed that the pion cross sections asymptotically approach an exponential decrease with increasing pion energy. The limiting slope becomes systematically less steep with increasing beam energy and with increasing mass at a given beam energy.

I will restrict my discussion for the most part to the hills and valleys in heavy ion pion spectra that show up at the lower pion energies.

We shall examine the following:

I. Three kinds of funny hills

II. $\pi^-/^+$ ratios near center of mass

III. New Monte Carlo studies of charged pion spectra

IV. Pion orbiting about fireballs and Bose-Einstein behavior as explanation for the mid-rapidity $P_\perp \approx 0.4 - 0.5\ m_\pi c$ hill.

THREE KINDS OF FUNNY HILLS

We first examine the main π^+ hills observed by our TOSABE (TOkyo-OSaka-BErkeley) collaboration using a scintillation range telescope on the ^{20}Ne + NaF system. Fig. 1 from this work[1] shows a main peak in the backward direction at a rapidity of -0.4. Of course, by symmetry there must be a corresponding forward peak. These peaks are closely analogous to those seen by Cochran et al.[2] in $p + p = \pi^+ + X$ at 730 MeV. These peaks are explained in the isobar model as the decay of aligned $\Delta(1232)$ resonances of spin 3/2. For Ne + NaF at 400A MeV the peak has pulled in to near target rapidity but we may still attribute the peak to decay of a $\Delta(1232)$, now virtual. We called attention to a second kind of funny hill in the 800A MeV data involving much slower pions (c.m.) and situated near 90° (c.m.) at ~ 0.5 $m_\pi c$ momentum. This funny hill of the second kind did not appear in 400A MeV data,[3] as is evident in Fig. 1. We will not comment on the Pb target data in Fig. 1.

About the same time that we reported the neon data Wolf et al.[4] reported the funny hill of the second kind also in ^{40}Ar + Ca at 1.05A GeV. Fig. 2 here shows our computer-drawn contour plots using their range telescope data alone (lower half) and combining their data (solid dots show locations of their data points, with open circles the symmetry-reflected points) with our magnetic spectrometer data[3] (upper half, with our 70 data bins lying within the bold line enclosing our spectrometer acceptance. Now there are some minor differences on a couple of data points in the region where the edge of our acceptances overlap, though for most of the overlap we have remarkable agreement. Their data alone suggest a ridge, but combined with ours there seems to be more an undulating plateau. At any rate the feature goes out in $P_\perp$ to about 0.4 $m_\pi c$ and seems surely to be analogous to what we called a funny hill of the second kind in the Ne data.

Note that the funny hill of the first kind, the Δ-decay peak, seems to be washed out in the Ar data. We suggest that its absence is a consequence of more rescattering of pions in the greater mass system.

We next consider the sharpest and most dramatic feature, the π^- peaks near beam velocity. To follow the chronological order of their first observation I shall call them for this talk funny hills of the third kind. Their thorough investigation is the subject of a forthcoming publication.[6] I will just show one example from yet more recent work.[7] In Fig. 3 we see isometric and contour plots of the Lorentz-invariant cross-section for π^- in Ne + NaF at 138A MeV. The π^+ spectra always show a depression near beam velocity. We believe the π^- peak and π^+ hole are consequences of Coulomb focussing by projectile fragments. Quantitative fits on this basis are made by Radi et al.,[8] in which the primary fragment distribution and momentum dispersions of compound nuclei before nucleon evaporation play the central role.

Gyulassy and Kaufmann[9] have given treatments of the Coulomb focussing effects and fit our earlier data[10] with a model of thermally expanding fireball and spectators (cf. their Figs. 2 and 6). Their spectator temperature parameter should, in light of later work,[8] not be regarded literally but rather as a parameter that mocks up the momentum dispersion of bound projectile fragments.

Libbrecht and Koonin[11] also studied the Coulomb effect on pions. They not only attributed the beam velocity π^- peak (hill of the third kind) to Coulomb effects but also the low energy mid-rapidity π^+ peak (hill of the second kind) to Coulomb effects. To reproduce data of Wolf et al.[3] they needed to postulate some nuclear charge strung out on the line between fragments. As we shall show in a later figure, the hill of the second kind also occurs in π^- spectra, thus making a pure Coulomb explanation implausible.

π^-/π^+ RATIOS NEAR CENTER OF MASS

In subsequent work Cugnon and Koonin[12] restudied the pion Coulomb problem by Monte Carlo methods with relativistic trajectories. Their plot of π^-/π^+ ratios at 0° for the Ar^{40} on Ca^{40} collision at 1.05A GeV shows the familiar beam velocity peak ("third kind") but in addition a secondary peak at rest in the center-of-mass. Their π^-/π^+ ratio is about 5.5 at the center-of-mass.

Our group* then measured both π^- and π^+ spectra at and near rest in the c.m. frame for 1.05A GeV ^{40}Ar on natural C, Cu, and U targets. The spectra along the 16° (lab) angle are shown in Fig. 4. The spectra are seen to be quite flat except for π^- from the uranium target. Furthermore, this flatness holds over the whole region of our spectrometer acceptance (shown in Fig. 2) including the nucleon-nucleon center of mass.

In Table I are summarized the π^-/π^+ measured values at the nucleon-nucleon center-of-mass.

TABLE I
π^-/π^+ Ratios at the Nucleon-Nucleon c.m.
for Heavy Ion Collisions

Lab Energy per Nucleon (MeV)	Projectile	Target	π^-/π^+ Ratio at c.m. (± 10%)
1050	^{40}C	C	1.6
		Cu	1.5
		U	3.2
655	^{20}Ne	NaF	1.76

NEW MONTE CARLO THEORETICAL STUDIES

Faced with the large discrepancy between theory and experiment for π^-/π^+ ratios, Radi, Frankel, Sullivan and I undertook, a new Monte Carlo study of pion trajectories. Before the Monte Carlo work we examined approximate analytical as well as numerical solutions for some simple special cases. We considered first at time zero two touching nuclei of equal charge with a pion emitted from the point of tangency. Whether treating the axially symmetric case (physically unrealistic but mathematically simple) or the case of a grazing impact parameter equal to a nuclear diameter, the classical Jacobian factors for very slow pions remain near unity for both π^- and π^+. This result contrasts strongly with the result of expressions in Ref. 9, where the Coulomb

*Principal collaborators on our JANUS magnetic pion spectrometer measurements at midrapidity have been the following: James Bistirlich, Harry Bowman, Roy Bossingham, Kenneth Crowe, Kenneth Frankel, Jeff Martoff, James Miller, Don Murphy, John Rasmussen, John Sullivan, William Zajc and Eunice Yoo, U.C. Lawrence Berkeley Laboratory; Osamu Hashimoto and Masahiro Koike, Institute for Nuclear Studies, University of Tokyo; Jean Quebert, University of Bordeaux; Walter Benenson, Gary Crawley, Edwin Kashy, and Jerry Nolen, Michigan State University; and Jean Péter, Laboratory for Nuclear Research, Orsay.

contributions of different charge centers add as scalar terms, depending on magnitude but not on direction of the relative velocity vector between the pion and each charge center.

For unequal nuclear charges the cancellation is considerable but not complete, and Fig. 5 shows the calculated in-plane velocity shift field for $^{40}_{18}Ar$ (below) and $^{40}_{20}Ca$ (above) in a grazing collision at 1.05A GeV (lab). The shifts are seen to be quite large, making perturbative approximations impractical. By stepping the initial velocity by small increments the classical Jacobians were evaluated. The number by each arrowhead is the ratio of π^-/π^+ Jacobians for given initial velocity (to compare with experiment one would need the ratio for given final velocity). The ratio in italics by the middle of each arrow is taken from the approximation of the Jacobian out to the first order term, the divergence of the velocity shift field. This approximation is seen not to be very good.

In order to compare with available pion inclusive data a more complicated calculation must be done, averaging over impact parameters. Pions will not always originate on the mid-point between charge centers, and cancellation of Coulomb effects for slow pions will, as we shall see, be not so complete as for grazing cases.

Fig. 6 shows schematically three different stages of a heavy ion collision at intermediate impact parameter. For our Monte Carlo calculations the very complex situation had to be reduced to a practical model. Principal differences we wished to test relative to the Cugnon and Koonin work[12] were the following: (1) the pions should originate from the surface, not throughout the collision volume, (2) those trajectories that passed through nuclear matter should be rejected due to pion reabsorption, (3) the pions should be emitted at the time of closest approach, not the late stage of the collision and (4) a two-fireball thermal plus first-collision source for initial pion momentum distribution was taken, rather than a single thermal source.

We initially anticipated a high degree of cancellation of Coulomb effects on low energy pions by the participant protons expanding faster in all directions. Thus, the Monte Carlo calculation was carried out considering only spectator charges left after geometrical scraping out of participants. The initial position was selected randomly along a quadrant of the intersection ring of the original nuclei. The initial momentum was selected from a distribution flat in momentum space (the two-fireball source function was brought in at a later stage as a weighting function in binning final momenta). Fig. 7 gives a scatter plot of initial and final velocities of surviving (not absorbed or orbiting) trajectories for π^-, π^+, and π^0 for Ne + Ne at 655A MeV (lab) at an intermediate impact parameter. The initial and final distributions of π^0 are, of course, the same, since there is no Coulomb deflection. There is absorption to cause some modification from the initial flat distribution. The dot densities increase linearly with $v_\perp$ because of the geometrical effect of projecting from three-dimensional velocity space onto a two-dimensional plot. The initial distribution of surviving π^- orbitals shows empty regions about the beam and target velocity corresponding to trajectories lost to absorption or orbiting. (Orbiting in these low-Z systems does not correspond to pionic atom orbits, since the orbital angular momenta are much

less than $\hbar$). There is a slight forward-backward asymmetry, since initial pion positions were selected on just the forward quadrant. For final results the forward and backward velocities (c.m.) are folded together, giving the required symmetry. The final π^- points show a bunching near beam and target velocities. The final π^+ points show complete exclusion from regions about beam and target velocities, a result of classical Coulomb repulsion.

Since pion reabsorption is a principal difference of our calculation from that of Cugnon and Koonin,[12] it is of interest to observe in Fig. 8 the fraction of surviving trajectories as a function of impact parameter. (We assumed absorption if the trajectory passed within 0.8 nuclear radius of a spectator center. The number 0.8 is rather arbitrary.)

The next several figures show final results after weighting with a two-fireball source function and impact-parameter averaging. Fig. 9 shows "vertical" slices, i.e. differential cross-sections vs. $v_\perp$ for ranges of $v_\parallel$, for π^-. Data of Ref. 6 for 90° c.m. are plotted for comparison. The flatness of data and theory along 90° c.m. are evident. The peak at beam velocity is seen in the lowest band. Fig. 10 shows a "horizontal" slice, the cross-sections along 0°. The beam velocity π^- peak is seen, and a small bump at intermediate velocity is given by theory and perhaps shown by the data. To get some insight into this unexpected bump we examine Fig. 11, which separates the contributions of three regions of impact parameter. The new bump seems to come from intermediate impact parameters and may be some subtlety of the 3-body Coulomb system and particular ring radius for injection of the π^-. Its nature is too uncertain to dignify the new bump as a "hill of the fourth kind."

Fig. 12 shows the vertical slices for the π^+ spectra, with the 90° c.m. data plotted for comparison.

Fig. 13 is the corresponding 0° spectrum for π^+. It is seen that the theory much exaggerates the π^+ hole compared to experiment. This problem is likely a consequence of our neglect of quantum mechanics; tunneling would allow some π^+ in the classically forbidden part of velocity space near beam velocity.

We now apply these Monte Carlo results to the problem of the π^-/π^+ ratio near rest in the c.m. Besides the spectator Coulomb factor we have to consider the effect of the 5% neutron excess in NaF. Also the participant charge cannot be strictly ignored, since in our model the pions do not start from the origin but from the intersection ring. We have not attempted a general solution of the participant charge effect but have derived the Coulomb contribution for the special case of zero-energy (c.m.) pions. Table II summarizes the three factors and their product, the theoretical π^-/π^+ ratio.

TABLE II
Zero Energy (c.m.) π^-/π^+ Ratio Factors

	^{20}Ne+NaF at 655A MeV	^{40}Ar+Ca at 1050A MeV
Spectator Coulomb factor	1.40	1.36[a]
Neutron-excess factor	1.083	1.17
Participant Coulomb factor	1.11	1.10
Final Product (theory, Ref. 13)	1.68	1.75
Experiment (Ref. 5)	1.76 ± 0.1	1.5 ± 0.2

[a]Calculated by scaling from Ne Monte Carlo results.

The Coulomb factors are expected to scale roughly as $ZR^{-1}\ k_{\pi c.m.}^{-2}$, and thus in Table II they are slightly smaller for the argon system than for neon due to the higher energy of the former. The above scaling rule from Ref. 13 is specialized to symmetric collisions, with Z the charge, R the nuclear radius, and $k_{\pi c.m.}$ the wave number of a pion at rest in the c.m. evaluated in the lab frame. The final agreement in Table II is satisfactory, considering the many approximations in the theory. We have taken a great deal of this paper to describe the new Monte Carlo trajectory work, which might seem a diversion from the "funny hills" theme. However, besides addressing the π^-/π^+ ratio at the origin the new work has shown spectator Coulomb effects not to be responsible for hills other than the π^- peak near beam velocity and possibly the 0° bump at 0.1 $m_\pi c$. This general flatness result was not trivially to be expected, since celestial mechanics contains peculiarities in the > 3-body problem such as Trojan points of stability, the shepherding moon behavior around Saturn, etc. Furthermore, the theory in both Refs. 11 and 12 suggested other hills due to Coulomb effects.

POSSIBLE PION ORBITING ABOUT FIREBALL(S)

In this talk I have deferred until now showing fully the data that really convinced us that the mid-rapidity hills of the second kind did not have a trivial Coulomb explanation. Only 0° and 90° c.m. cuts of these data were shown on the Monte Carlo plots just preceding.

In Figs. 14 and 15 you see isometric and contour plots of the π^- invariant cross-sections for Ne plus NaF at 655A MeV. The highest peak (upper-right hand corner) is the now-familiar beam velocity peak (hill of the third kind). However, there is new structure at mid-rapidity, with the cross-section peaking above 3 b $sr^{-1}GeV^{-2}$ at 90° c.m. and 0.4 $m_\pi c$ momentum. The π^+ funny hill of the second kind reported in Refs. 1 and 4 has its counterpart in π^-! It is thus highly unlikely that there is a simple Coulomb explanation for the 90° c.m. hills of the second kind. In Fig. 16 we show the contour plot of

our π^+ data for the same system and in Fig. 17 the cuts along 90° c.m. We did not have sufficient beam time to measure far enough out along the 90° c.m. line to cover the bump region, but the data are consistent with such a bump for π^+ as well as π^-. For π^- we show in the solid line a comparison with work of Nagamiya et al.[14] This line represents an interpolation in beam energy between 400A MeV and 800A MeV, and it represents an extrapolation down in pion energy. Their lowest measured pion point would be on the right margin of Fig. 17, and the extrapolation follows a Boltzmann form, Gaussian in momentum, exponential in energy.

At the high-momentum edge where the two data sets nearly overlap our data appear to be approaching theirs. At the origin the extrapolation from the Nagamiya work matches our data, and the nature of the hill of the second kind is delineated. The excess cross-section above the extrapolated line forms a broad hill from 0.4–0.6 $m_\pi c$ dropping to zero above and below this momentum region.

What could be the significance of this mid-rapidity hill? It suddenly occurred to me a few months ago that simple application of the uncertainty principle to this ubiquitous momentum of ~ 0.5 $m_\pi c$ gives a distance of ~ 2 pion Compton wavelengths, or ~ 3 fm. This distance is around the size expected for the hot fireball source region. Zajc et al.[15] report the following source radii deduced from 2-pion correlations from 1.8A GeV ^{40}Ar on KCl. From $2\pi^-$ data they deduce R = 3.12 ± 0.33 fm, and from $2\pi^+$ data, R = 3.92 ± 0.43 fm.

The boson properties of like pions should give them a tendency for enhanced filling of the lowest quantum state in a box. Prior theoretical papers have pointed out the possibility of a "zero-energy" pion component in thermally equilibrated pions from heavy ion collisions. Kitazoe and Sano[16] solved equations of thermal equilibrium for nucleons and pions in mass-40 collisions for various beam energies. The pion chemical potential is always negative but approaches zero at intermediate beam energies, thus giving an optimum beam energy for fraction of pions that are boson-condensed as "zero-energy" pions. Zimanyi, Fai, and Jakobsson[17] similarly derived theoretical pion spectra and give a boson-condensed component. They plot the condensed component not as a zero-energy delta function but as of finite width of a few MeV, consistent with the uncertainty principle. They stress that the boson-condensed pions are a distinct phenomenon and are not the virtual pions of "pion condensation" of the Migdal-Sawyer kind. I would like to see more theoretical attention to this point, however. There is an implicit assumption in Ref. 17 that the hot nuclear matter blob provides an attractive potential with a lowest bound state for pions.

The data on the mid-rapidity bumps generally peak away from zero (c.m.) momentum. Let us assume the bump data are snapshots of the boson-condensed pion wave function in momentum space. By elementary quantum mechanics the Fourier transform should give us the wave function in configuration space.

The mid-rapidity bump in the neon measurements could be approximated by a 1p harmonic oscillator wave function. Inclusive measurements cannot tell us whether the wave function is toroidal, i.e. cylindrically symmetric about the

beam axis, or dumb-bell-shaped lying in or out of the reaction plane. Let us assume a dumb-bell shaped p-wave functions with lobes perpendicular to the reaction plane. The wave function in both of the other directions will be a simple Gausian in either momentum or configuration space. In the third direction the configuration-space wave function dependence is

$$Y(y) = Ny \exp(-y^2/2r_o^2)$$

The sine Fourier transform of this gives the momentum space wave function

$$F(k_y) = N\pi^{1/2} r_o^2 k_y \exp(-k_y^2 r_o^2/2)$$

The maximum value of the former is at $y_1 = r_o$ and of the latter at $k_1 = r_o^{-1}$. This result is exactly the same as we gave intuitively earlier from the uncertainty principle. A momentum maximum of $p_1 \approx 0.5\ m_\pi c$ means $r_1 \approx 3$ fm. At this distance r_1 from the collision axis is the maximum probability of the transiently occupied π-orbital in the neon system. It is probably pushing the data too far to infer a size along the beam direction from the extent of the momentum bump in the $p_\parallel$ direction. However, the half width in momentum in the parallel direction seems less than half the perpendicular p_1 value. This would imply a parallel distance in the pion wave function of 6 or 7 fm.

The Ar data are not so clearcut, as there are unresolved differences between the independent measurements. Qualitatively, the analysis gives similar distances, perhaps a little shorter in the parallel direction and a bit longer in the perpendicular.

How can such orbitals form, and why is a p-orbital, instead of the lowest s-orbital apparently occupied? We note that a slow-moving pion in the fringe region of an expanding nuclear fireball (or two) should receive a binding contribution from the p-wave interaction with nucleons streaming by it during the expansion. The absorption process, whereby the pion vanishes and gives its rest-mass energy to two nucleons, may be weak in the fringing region, where nucleon density in phase space may be relatively low. By the same token an s-wave function may be less favorable from both standpoints — poorer binding from outward-streaming nucleons and stronger true absorption. The problem calls for theoretical attention. A p-wave pion at 3 fm has ~ 15 MeV of centrifugal energy, so this order of hadronic binding energy is needed. Theoretical work might follow the lead of that of T. Ericson and F. Myhrer[17] and of Mandelzweig et al.,[18] who calculate binding of pion s-states in nuclei. These works, dealing with unexcited nuclei, indeed show bound states but with such large absorption widths as to be unobservable. Perhaps the heavy ion collision provides for a fleeting instant a suitable environment for such pion bound states, and their boson properties enhance the occupation of these states.

This work was supported by the Director, Office of Energy Research, Division of Nuclear Physics of the Office of High Energy and Nuclear Physics of the U.S. Department of Energy under Contract DE-AC03-76SF00098.

References

1. K. Nakai, J. Chiba, I. Tanihata, M. Sasao, H. Bowman, S. Nagamiya, and J. O. Rasmussen, Phys. Rev. C 20, 2210 (1979).

2. D. Cochran, P. Dean, P. Gram, E. Knapp, E. Martin, D. Nagle, R. Perkins, W. Shlaer, H. Thiessen, and E. Theriot, Phys. Rev. D 6, 3085 (1972).

3. J. Chiba, K. Nakai, I. Tanihata, S. Nagamiya, H. Bowman, J. Ingersoll, and J. O. Rasmussen, Phys. Rev. C 20, 1332 (1979).

4. K. L. Wolf, H. H. Gutbrod, W. G. Meyer, A. M. Poskanzer, A. Sandoval, R. Stock, J. Gosset, C. H. King, Nguyen Van Sen, and G. D. Westfall, Phys. Rev. Lett. 42, 1448 (1979).

5. K. A. Frankel, J. A. Bistirlich, R. Bossingham, H. R. Bowman, K. M. Crowe, C. J. Martoff, D. Murphy, J. O. Rasmussen, J. P. Sullivan, W. A. Zajc, J. P. Miller, O. Hashimoto, M. Koike, J. Peter, W. Benenson, G. M. Crawley, E. Kashy, J. A. Nolen, Jr., and J. Quebert, Phys. Rev. C 25 1102 (1982).

6. J. P. Sullivan, J. A. Bistirlich, H. R. Bowman, R. Bossingham, T. Buttke, K. M. Crowe, K. A. Frankel, C. J. Martoff, J. Miller, D. L. Murphy, J. O. Rasmussen, W. A. Zajc, O. Hashimoto, M. Koike, J. Péter, W. Benenson, G. M. Crawley, E. Kashy, and J. A. Nolen, Phys. Rev. C 25, 1499 (1982). Also J. P. Sullivan, Ph.D. Thesis, Univ. of Calif., Berkeley, LBL Report 12546 (1981) unpublished.

7. D. Murphy J. Bistirlich, H. Bowman, R. Bossingham, K. Crowe, O. Hashimoto, K. Frankel, J. Rasmussen, J. Sullivan, W. Zajc, J. Péter, W. Benenson, G. Crawley, E. Kashy, and J. Nolen, Bull. Am. Phys. Soc. 26, 1148 (1981).

8. H. M. A. Radi, J. O. Rasmussen, J. P. Sullivan, K. A. Frankel, and O. Hashimoto, Phys. Rev. C 25, 1518 (1982).

9. M. Gyulassy and S. K. Kauffman, Nucl. Phys. A362, 503 (1981).

10. W. Benenson, G. Bertsch, G. M. Crawley, E. Kashy, J. A. Nolen, Jr., H. Bowman, J. G. Ingersoll, J. O. Rasmussen, J. Sullivan, M. Koike, M. Sasao, J. Péter, and T. E. Ward, Phys. Rev. Lett. 43, 683 (1979).

11. K. G. Libbrecht and S. E. Koonin, Phys. Rev. Lett. 43, 1581 (1979).

12. J. Cugnon and S. E. Koonin, Nucl. Phys. A355, 477 (1981).

13. H. M. A. Radi, J. O. Rasmussen, K. F. Frankel, J. P. Sullivan, and H. C. Song, U.C. Lawrence Berkeley Laboratory Report LBL-13768 (submitted to Phys. Rev. C, 1982).

14. S. Nagamiya, M.-C. Lemaire, E. Moeller, S. Schnetzer, G. Shapiro, H. Steiner, and I. Tanihata, Phys. Rev. C 24, 971 (1981).

15. W. A. Zajc, J. Bistirlich, R. Bossingham, H. Bowman, C. Clawson, K. Crowe, K. Frankel, O. Hashimoto, J. Ingersoll, M. Koike, J. Kurck, C. Martoff, W. MacDonald, J. Miller, D. Murphy, J. Rasmussen, J. Sullivan, P. Truol and E. Yoo, Proc. 5th High En. Heavy Ion Study, Berkeley (May 18-21, 1981) LBL Report-12552, CONF-8105104.

16. H. Kitazoe and M. Sano, Lett. Nuovo Cim. 14, 400 (1975).

17. J. Zimanyi, G. Fai, and B. Jakobsson, Phys. Rev. Lett. 43, 1705 (1979).

18. T. E. O. Ericson and F. Myhrer, Phys. Lett. 74B, 163 (1978).

19. V. B. Mandelzweig, A. Gal, and E. Friedman, Ann. Phys. (N.Y.) 124, 124 (1980).

Figure Legends

Fig. 1 Contour plots of Lorentz-invariant π^+ production cross sections for six different systems. (From Ref. 1.) (Units of mb sr^{-1} GeV^{-2}.)

Fig. 2 Contour plots of Lorentz-invariant π^+ production cross sections for ^{40}Ar + Ca at 1.05A GeV. (Units of b sr^{-1} GeV^{-2}.) The lower figure is drawn from data of Wolf et al.[4] alone, dots indicating location of their data points. The upper figure is drawn from combined data of Refs. 4 and 5, with Ref. 5 acceptance region enclosed by the bold lines.

Fig. 3 Isometric and contour plots of π^- data[7] for ^{20}Ne + NaF at 136A MeV. Cross section is in units of b sr^{-1} GeV^{-2}. Peak is near beam velocity.

Fig. 4 Pion production cross sections by ^{40}Ar at 1.05A GeV at 16° (lab) for three targets, U, Ca, and C. Abscissa is pion kinetic energy in the laboratory frame.

Fig. 5 Map of velocity shift (for pions with $v_z = 0$) fields (c.m. frame) for grazing impact parameter for π^- (solid arrows) and π^+ (dashed arrows). The position of the ^{40}Ar nucleus is in the positive y direction with its velocity directed along the positive x axis. The numbers near the arrowheads are π^- to π^+ ratios of the classical Jacobians (phase space factors) calculated exactly from trajectory mapping. The italic numbers midway on the solid arrow are the corresponding ratios for the approximations $J = 1 - \nabla\cdot\delta\vec{v}$. It is not correct to equate these ratios with common initial velocity to π^-/π^+ Coulomb ratios, since the velocity shifts are so large. One would need to divide Jacobians at the same final velocity.

Fig. 6 Schematic sketches of heavy ion collision and pion production for three successive times (c.m.).

Fig. 7 Scatter plot of Monte Carlo initial and final $v_\parallel$ and $v_\perp$ values for trajectories surviving absorption or orbiting capture. Values are shown for one impact parameter 0.4 b_0 for the ^{20}Ne + ^{20}Ne system at 655 MeV/A (see text).

Fig. 8 Plot of the surviving percentage of Monte Carlo trajectories for the three different pion charges as a function of impact parameter.

Fig. 9 Histograms of the final Monte Carlo π^- vs. $\beta_{\pi\perp}$ for five different cuts of width 0.1 c. Uppermost is at c.m. and lowermost is centered about the beam velocity. Data from Sullivan's thesis are shown for comparison.[6]

Fig. 10 Cut along 0° for π^-. The theory is shown both by histogram and computer-smoothed curve. The width of the cut goes to 0.1 c, comparable to experimental resolution. Data are plotted with error

bars, and the theory has been normalized to the flat portion.

Fig. 11 Breakdown of the π^- theoretical spectrum of Fig. 10 for three ranges of impact parameter. Curve a is the most central with the ratio α of impact parameter to its maximum value ranging from 0.1-0.3 (instep of 0.1). Corresponding ranges for b and c are labeled on the figure.

Fig. 12 Same as Fig. 9 except for π^+.

Fig. 13 Same as Fig. 10 except for π^+.

Fig. 14 Same as Fig. 3 except for higher beam energy of 655A MeV.

Fig. 15 Flat contour plot of π^- for system in Fig. 14.

Fig. 16 Same as Fig. 15 except for π^+.

Fig. 17 Cuts of π^- and π^+ production cross sections for ^{20}Ne on NaF at 655A MeV. Upper half shows cut at 0°. The lower half shows the cut at 90° (c.m.) with comparison to data extrapolated from Nagamiya et al.[14] Lorentz invariant cross sections are in units of b sr^{-1} GeV^{-2}.

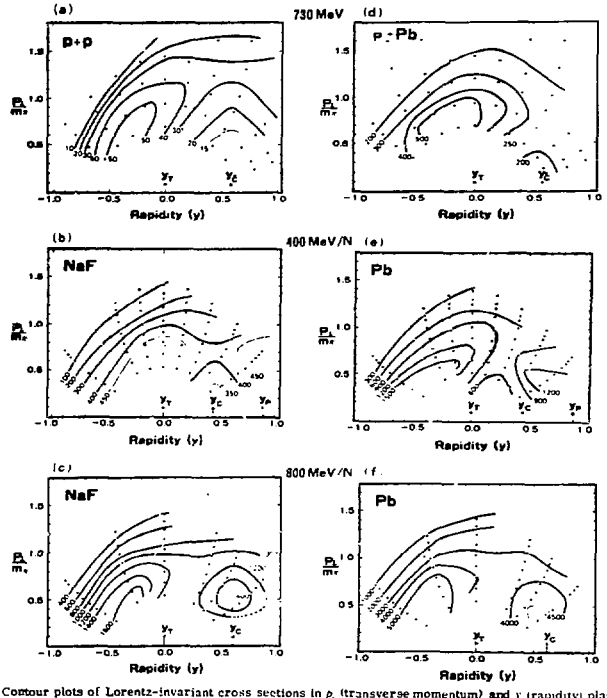

Contour plots of Lorentz-invariant cross sections in p_t (transverse momentum) and y (rapidity) plane for (a) $p+p$ at 730 MeV, (b) ^{20}Ne+NaF at 400 MeV/N, (c) ^{20}Ne+NaF at 800 MeV/N, (d) $p+$Pb at 730 MeV, (e) ^{20}Ne+Pb at 400 MeV/N, (f) ^{20}Ne+Pb at 800 MeV/N. The numbers written along contour lines are the Lorentz-invariant cross sections in units of mb sr^{-1} GeV^{-2} c. The dots indicate observed points.

XBL 808-11345

Fig. 1

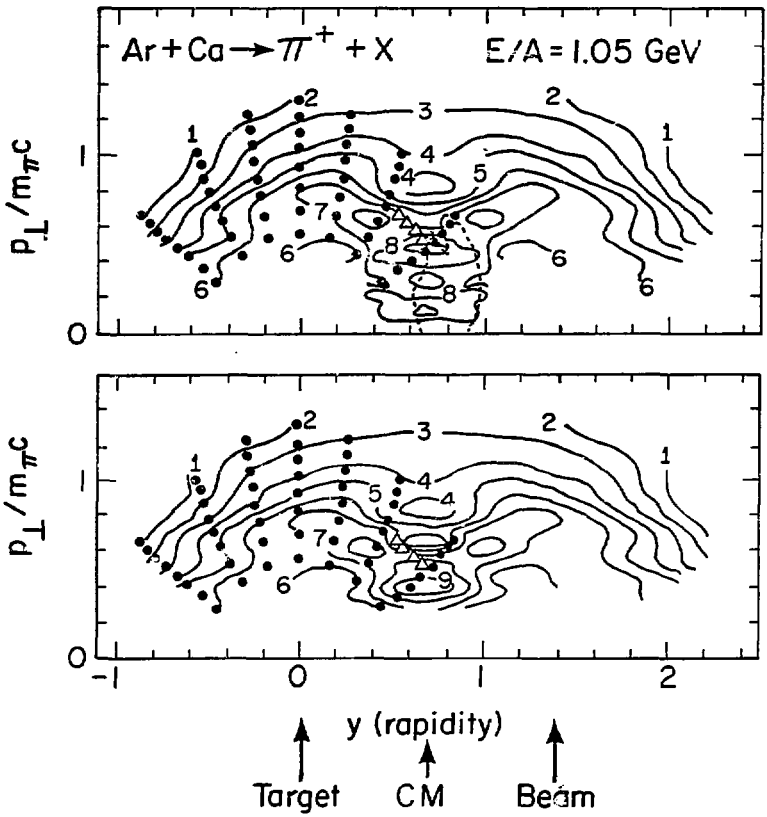

XBL 816-2375

Fig. 2

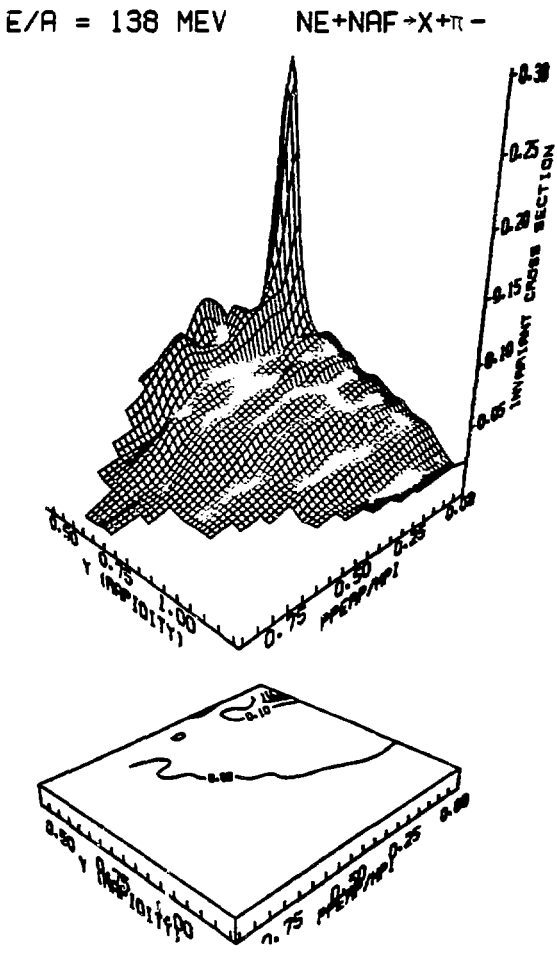

XBL 823-8269

Fig. 3

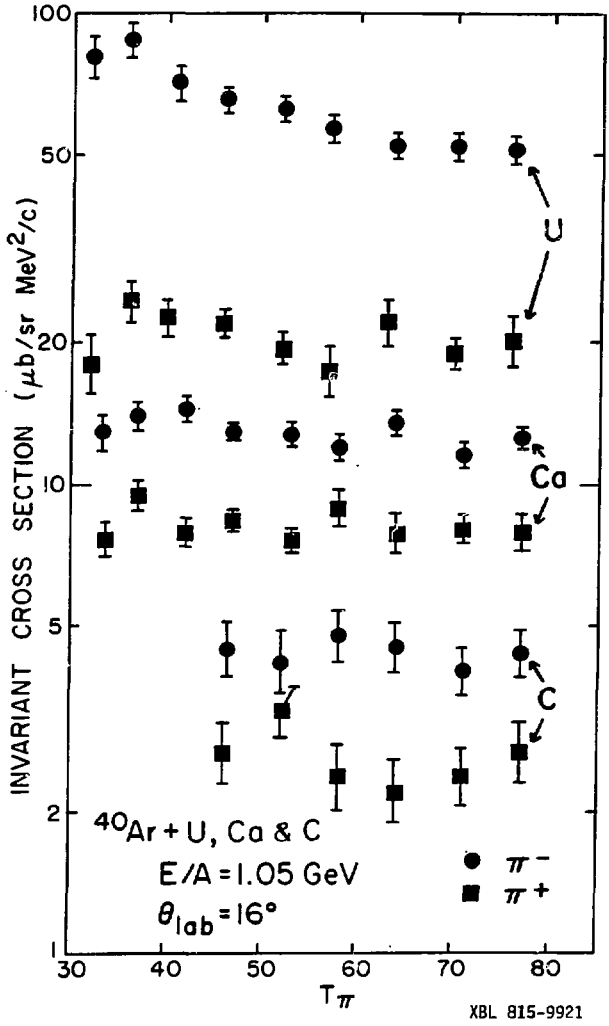
INVARIANT CROSS SECTION (μb/sr MeV²/c)
100
50
20
10
5
2
1
30
40
50
60
70
80
Tπ
U
Ca
C
40Ar + U, Ca & C
E/A = 1.05 GeV
θlab = 16°
π⁻
π⁺
XBL 815-9921

Fig. 4

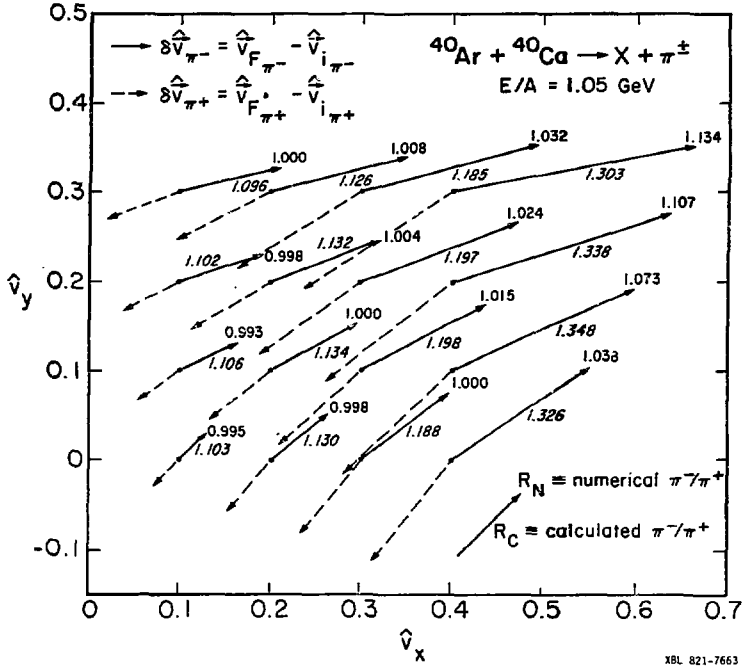
$\delta\hat{\vec{v}}_{\pi^-} = \hat{\vec{v}}_{F_{\pi^-}} - \hat{\vec{v}}_{i_{\pi^-}}$
$\delta\hat{\vec{v}}_{\pi^+} = \hat{\vec{v}}_{F_{\pi^+}} - \hat{\vec{v}}_{i_{\pi^+}}$
$^{40}Ar + ^{40}Ca \rightarrow X + \pi^{\pm}$
E/A = 1.05 GeV
$R_N \equiv$ numerical π^-/π^+
$R_C \equiv$ calculated π^-/π^+
$\hat{v}_y$
$\hat{v}_x$
XBL 821-7663

Fig. 5

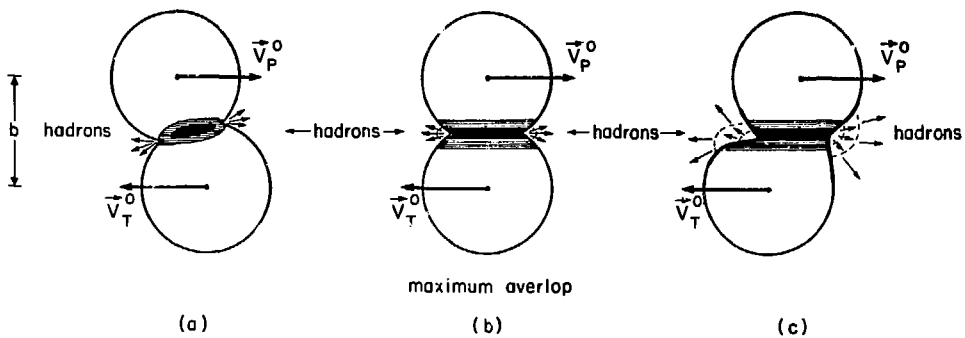

XBL 821-7657

Fig. 6

VELOCITY DISTRIBUTIONS OF SURVIVING PION TRAJECTORIES

$^{20}Ne + ^{20}Ne \rightarrow X + \pi$ E/A = 655 MeV b = 0.4 b_0

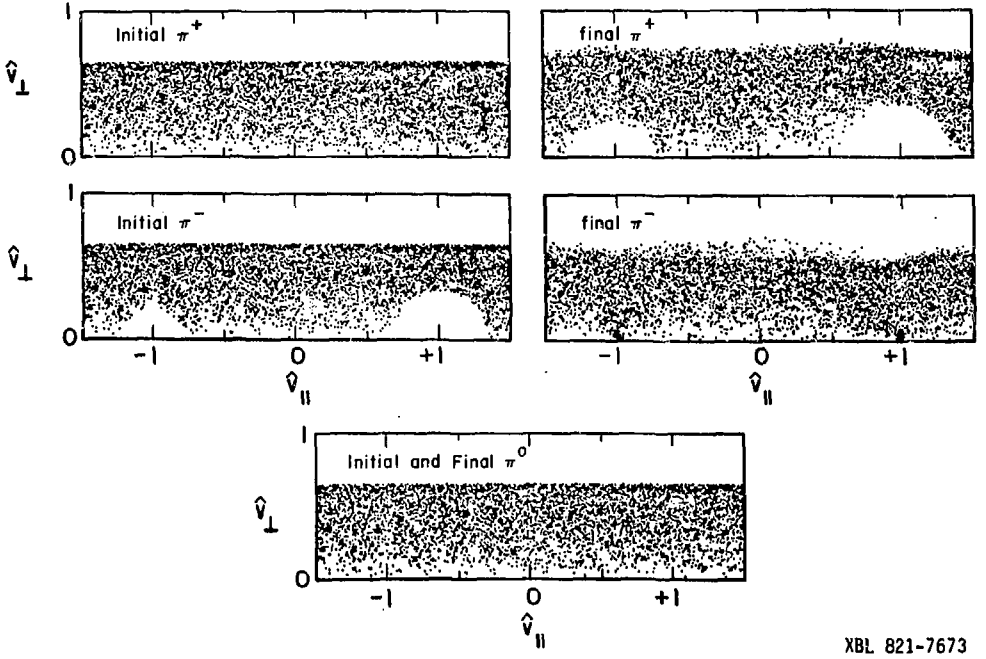

XBL 821-7673

Fig. 7

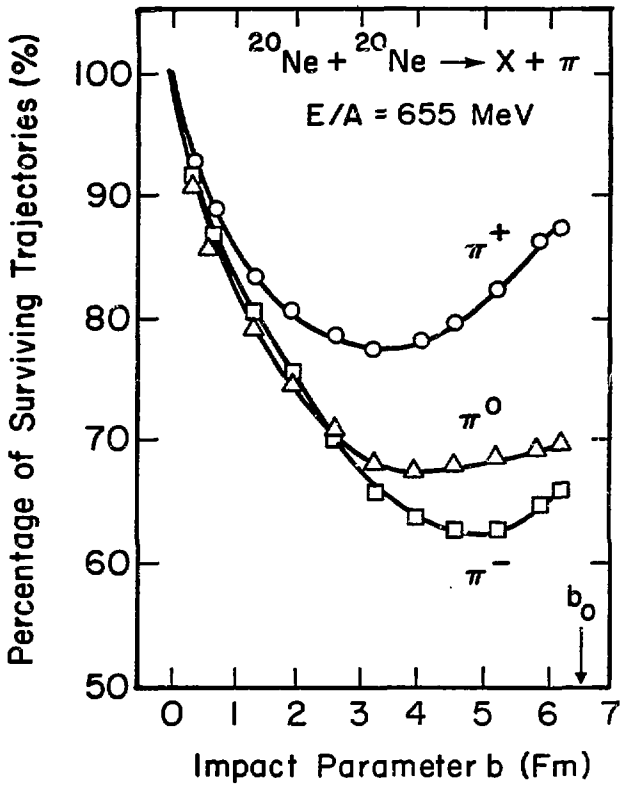

XBL 821-7672

Fig. 8

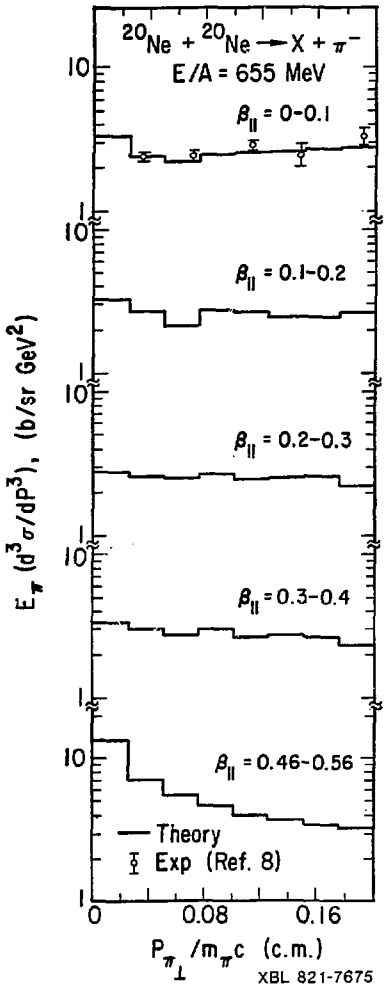
$^{20}Ne + ^{20}Ne \rightarrow X + \pi^-$
E/A = 655 MeV
$\beta_{\parallel}$ = 0-0.1
$\beta_{\parallel}$ = 0.1-0.2
$\beta_{\parallel}$ = 0.2-0.3
$\beta_{\parallel}$ = 0.3-0.4
$\beta_{\parallel}$ = 0.46-0.56
— Theory
Exp (Ref. 8)
$E_{\pi}(d^3\sigma/dP^3)$, (b/sr GeV^2)
$P_{\pi_\perp}/m_{\pi}c$ (c.m.)
XBL 821-7675

Fig. 9

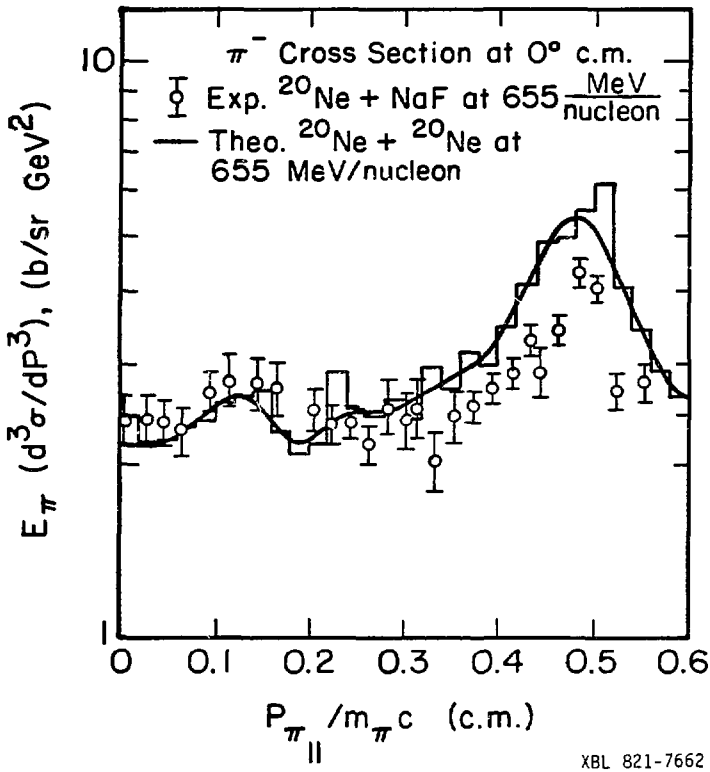
π⁻ Cross Section at 0° c.m.
Exp. 20Ne + NaF at 655 MeV/nucleon
Theo. 20Ne + 20Ne at 655 MeV/nucleon
10
1
0
0.1
0.2
0.3
0.4
0.5
0.6
Eπ (d3σ/dP3), (b/sr GeV2)
Pπ∥/mπc (c.m.)
XBL 821-7662

Fig. 10

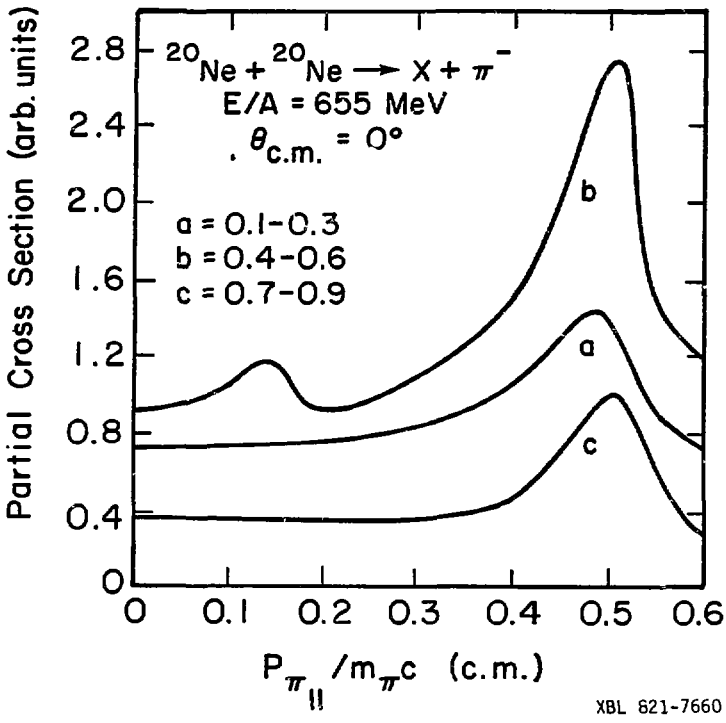
Partial Cross Section (arb. units)
2.8
2.4
2.0
1.6
1.2
0.8
0.4
0
$^{20}Ne + ^{20}Ne \rightarrow X + \pi^-$
E/A = 655 MeV
$\theta_{c.m.} = 0°$
a = 0.1-0.3
b = 0.4-0.6
c = 0.7-0.9
a
b
c
0
0.1
0.2
0.3
0.4
0.5
0.6
$P_{\pi_{\parallel}}/m_{\pi}c$ (c.m.)
XBL 621-7660

Fig. 11

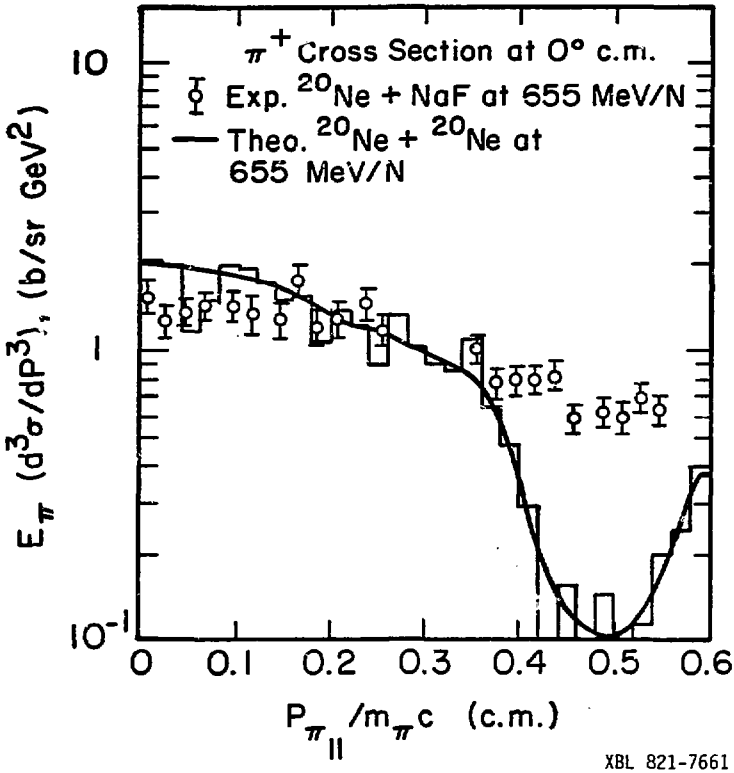

XBL 821-7661

Fig. 12

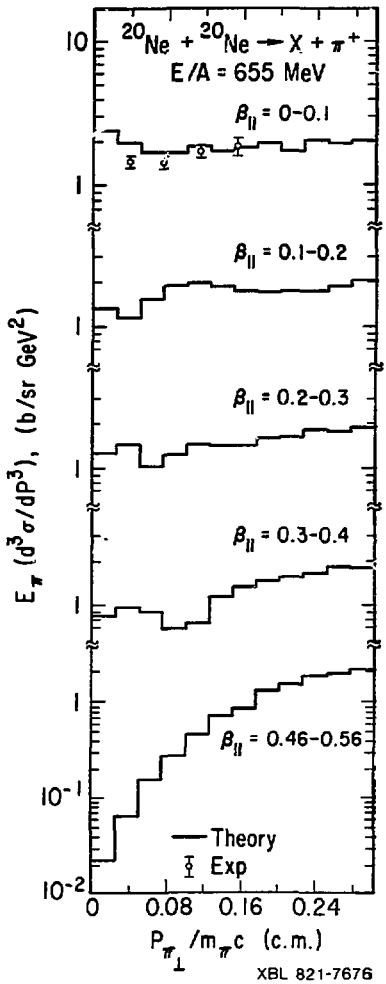
$^{20}Ne + ^{20}Ne \rightarrow X + \pi^+$
E/A = 655 MeV
$\beta_{\parallel}$ = 0-0.1
$\beta_{\parallel}$ = 0.1-0.2
$\beta_{\parallel}$ = 0.2-0.3
$\beta_{\parallel}$ = 0.3-0.4
$\beta_{\parallel}$ = 0.46-0.56
Theory
Exp
E_{π} ($d^3\sigma/dP^3$), (b/sr GeV^2)
$P_{\pi_{\perp}}/m_{\pi}c$ (c.m.)
XBL 821-7676

Fig. 13

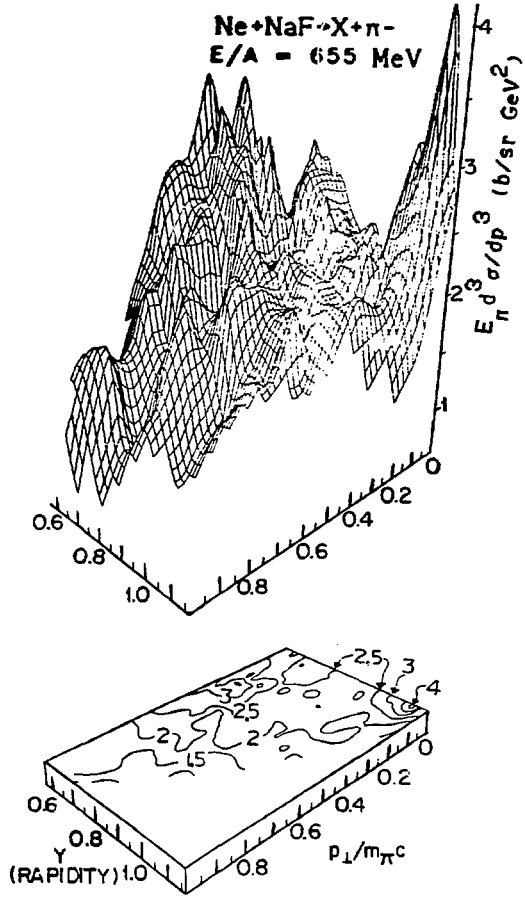

XBL8112-12886

Fig. 14

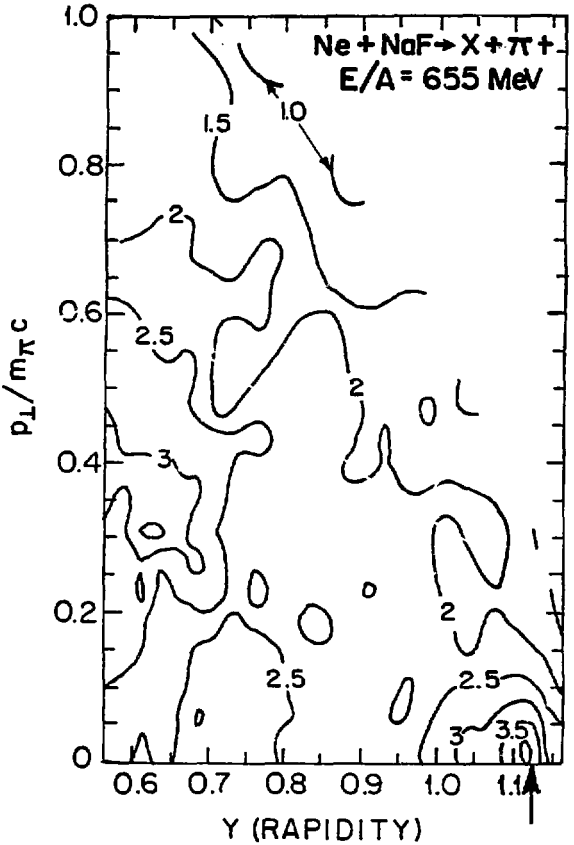

XBL 8112-12889

Fig. 15

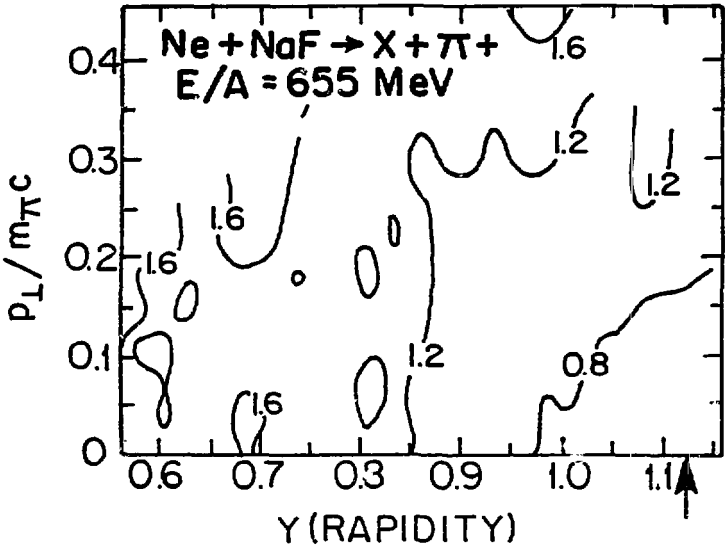

XBL 8112-12888

Fig. 16

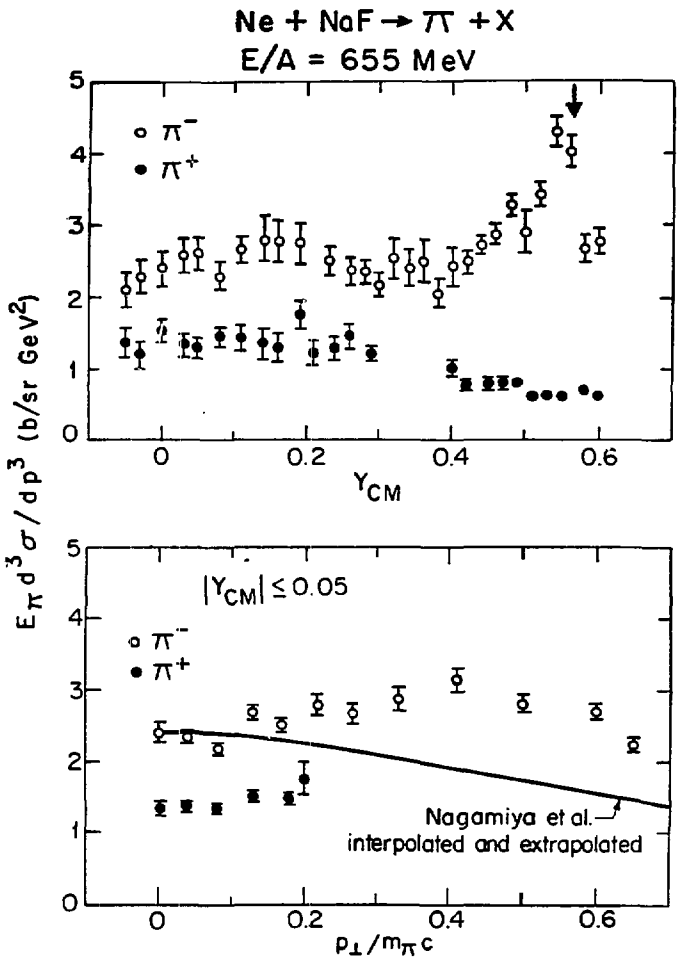

XBL 6112-12880

Fig. 17